Contrib Mineral Petrol (2007) 153:493–508
DOI 10.1007/s00410-006-0167-3

ORIGINAL PAPER

Tourmaline nodules from Capo Bianco aplite (Elba Island, Italy): an example of diffusion limited aggregation growth in a magmatic system

Diego Perugini · Giampiero Poli

Received: 20 November 2005 / Accepted: 29 November 2006 / Published online: 22 December 2006

Abstract The morphology of tourmaline nodules occurring in the Capo Bianco aplite (Elba Island, Italy) is studied. Outcrop features indicate that tourmaline nodules are the product of magmatic crystallization, as they are aligned along flow fields developed within the magmatic hosting mass. Mesoscopic observations indicate that nodule morphologies are very variable, from rounded to dendritic. Morphometric analyses show that tourmaline nodules are fractals and that fractal dimension quantifies their degree of irregularity. Numerical simulations of nodule growth are performed by using a Diffusion-Limited Aggregation process. The presence in natural samples of nodules with different morphologies is explained by considering a chaotic magmatic system characterized by a complex interplay between growth rate in different dynamical regions, latent heat of crystallization, and local convection dynamics. It is suggested that higher growth rates correspond to growth of tourmaline nodules in dynamical regions where the transfer of nutrients is very efficient. In such conditions, the latent heat released by the growing nodule is high, inducing strong local convection dynamics, destabilizing the nodule interface, and promoting the formation of dendritic morphologies. On the contrary, the growth of nodules in dynamical regions characterized by weak transfer of nutrients is inhibited leading to weak local convection dynamics and, consequently, to the formation of rounded morphologies.

Keywords Tourmaline nodules · Granitoid magmas · Fractal analysis · Diffusion-limited aggregation · Numerical simulation

Communicated by B. Collins.

D. Perugini (✉) · G. Poli
Department of Earth Sciences, University of Perugia,
Piazza Università, 06100 Perugia, Italy
e-mail: diegop@unipg.it

Introduction

A rich variety of patterns and morphologies have been described in all scientific fields, from biology to fluid dynamics, and intense research was carried out to develop more and more refined methods for analysing the complexity of natural shapes (e.g. Ottino et al. 1988; Chaplain et al. 1999). The presence of an interminable number of patterns and morphologies is also inherent to the field of igneous, metamorphic, and sedimentary petrology, where the interplay of a number of factors including temperature, pressure, concentration, etc. may act to produce extremely variable combinations of interlocking crystals resulting in an extraordinary amount of textures. In particular, regarding the field of igneous petrology, which is the field of interest in this contribution, intensive and extensive parameters may act jointly or independently to originate spectacular textures, such as those given by the rapid quenching of lavas in which dendritic, acicular, skeletal, and many other crystal morphologies can be observed (e.g. Cashman 1993; Faure et al. 2003). The important point about igneous textures is that the different crystal morphologies record the physicochemical conditions under which they crystallized and, hence,

they contain crucial information about the evolution of the magmatic system.

In this contribution we study tourmaline nodule morphology occurring in the aplitic rocks of Capo Bianco (Elba Island, Italy). The variable morphology of these nodules is analysed by fractal analysis and numerical simulations of Diffusion-Limited Aggregation are performed to simulate nodule growth. A model is advanced to explain the origin of the variable morphologies of natural samples.

Tourmaline nodules from Capo Bianco aplite (Elba Island, Italy)

Capo Bianco aplite crops out in central Elba Island as adjacent caps on a ridge (Fig. 1), interpreted as an original sill dismembered by younger intrusions. The outcrops make up a structurally higher tourmaline-rich laccolith layer (Westerman et al. 2000). It is a white porphyritic rock with alkali feldspar granite composition (Dini et al. 2002, 2006). Whole rock-muscovite Rb–Sr isochrons yielded cooling ages of 7.91 ± 0.1 Ma (Dini et al. 2002). Details and extensive discussion about geology and magmatic evolution of Elba Island complexes can be found in Dini et al. (2002).

Figure 2a and b show general views of Capo Bianco outcrop that appears as a ''leopard-skin'' in which dark tourmaline nodules with schorl-elbaite solid solution composition (Dini et al. 2006) are dispersed within the light coloured micro-granitoid mass. The outcrop is characterized by an inhomogeneous distribution of tourmaline nodules as evidenced by the occurrence of a broad rhythmic layering constituted by zones in which tourmaline nodules are scarce and zones in which they are more abundant. Figure 2b also shows that the granitoid mass is deformed by magmatic flow fields generating lamellar structures along which tourmaline nodules are aligned. A more detailed observation reveals that the host rock is constituted by two different lithotypes having white and pink colours (Fig. 3; light grey and dark grey, respectively, in the figures). The white coloured one in constituted only by light coloured minerals (plagioclase, K-feldspar, and quartz) whereas the pink coloured contains the same minerals plus muscovite and biotite. There is no variation in the grain size in the two lithotypes in that they both are fine-grained. Figure 3a–d show that the white and pink portions are intimately intermingled as evidenced by the presence of lamellae from the meter to the millimetre length-scale. Tourmaline nodules follow the structure of flow fields as evidenced by the fact that they are found aligned along streamlines defined by magmatic lamellae and folds (Figs. 2b, 3a–c, d). In addition, in some cases, flow fields are found to fold around tourmaline nodules indicating that nodules where present during the motion of the magmatic mass (Fig. 4a). Sometimes, tourmaline nodules crosscut the contact between the white and pink lamellae (Fig. 4b).

Tourmaline nodules occur in both lithotypes (Figs. 2–4) and several of those occurring in the pink one display a white halo (Fig. 3b) around them with

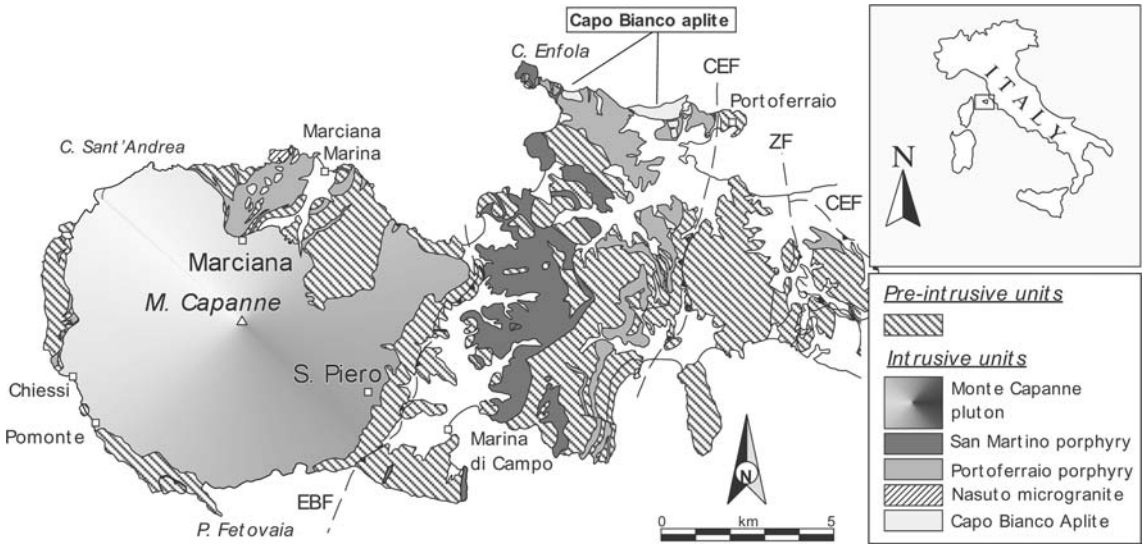

Fig. 1 Schematic geological map of Elba Island (central-western part) showing the location of Capo Bianco aplite outcrops (modified after Dini et al. 2002). Details on the intrusive and pre-intrusive units, and structural features, can be found in Dini et al. (2002) and here are not repeated

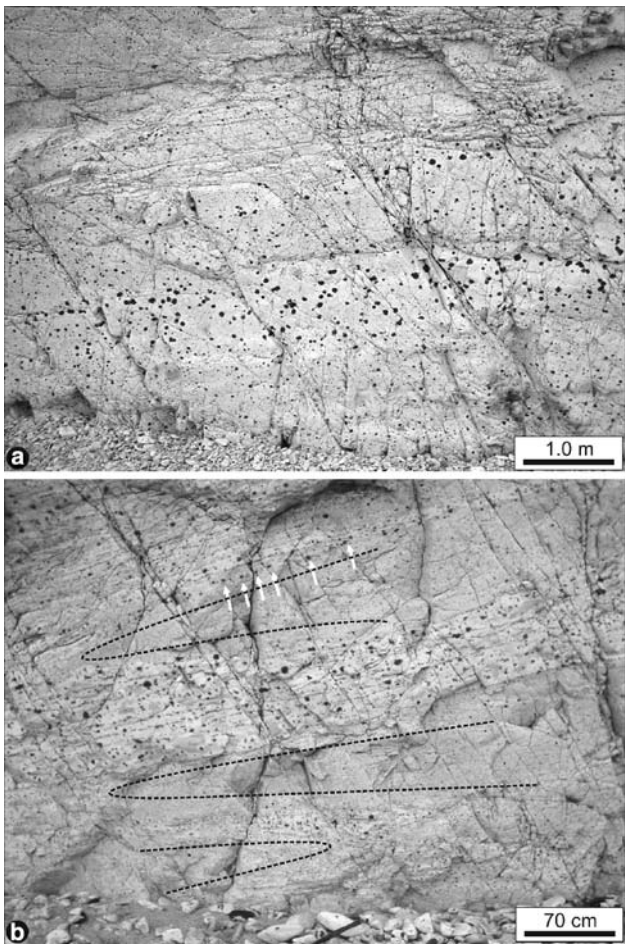

Fig. 2 General view of Capo Bianco outcrop showing the inhomogeneous layered distribution of tourmaline nodules in the light coloured aplitic rock (**a**) and the occurrence of lamellar and folded structures (*dotted lines*) along which tourmaline nodules are aligned (e.g. *white arrows*; **b**)

the same mineralogical composition of the white lithotype described above. Although several nodules display a white halo around them, several others do not (Fig. 3b).

From a morphological point of view, tourmaline nodules display extremely variable morphologies, from rounded to extremely irregular with fingers propagating radially from the centre of the nodule toward the host rock (Fig. 5). Such a morphological variability can be recognized in nodules occurring at short length scale, in some cases even in the same thin section. This morphological variability is present at all length scales, irrespective of the size of tourmaline crystals.

Thin section observations show that tourmaline nodules are constituted by a tourmaline framework including microcrystals (Fig. 6) mainly quartz, k-feldspar, and rare muscovite. Petrographic analysis indicates that each tourmaline nodule behaves optically as an individual crystal, as whole nodules go into extinction simultaneously in cross-polarized light (Fig. 6). Therefore, nodules can be considered as constituted by a tourmaline geometrical framework grown optically as an individual crystal and characterized by many lacunae filled by microcrystals. Nodules do not display any internal zoning regarding both their petrographic texture and chemical composition (Dini et al. 2006). Additionally, nodules are compact and do not show the occurrence of voids, such as miarolitic cavities.

Hypotheses for tourmaline nodule formation

Three main hypotheses can be advanced to explain the origin of tourmaline nodules in granitoid rocks. The first suggests that nodules may result from postmagmatic metasomatic-hydrothermal replacement of previously crystallized granite by boron-rich fluids (e.g. Rozendaal and Bruwer 1995). The second suggests that nodules may be magmatic-hydrothermal features related to the separation and entrapment of B-rich fluids from coexisting granitic magma (e.g. Sinclair and Richardson 1992; Shewfelt et al. 2005). The third hypothesis is that nodules may result by crystallization from a B-rich granitoid magmatic mass. In the following we evaluate these three hypotheses and discuss them by considering geological and petrographic features observed at Capo Bianco outcrop with the aim to understand the conditions under which tourmaline nodules crystallized in the studied rocks.

Rozendaal and Bruwer (1995) studied the Cape Granite Suite (South Africa) and noted that tourmaline nodules are typically spherical in shape, but also form tube-like morphologies. These authors proposed that nodules can be interpreted as post-magmatic replacement features, and that they are genetically related to tourmaline veins which acted as 'feeders' for nodule development.

At Capo Bianco, tourmaline nodules do not display tube-like morphologies and there is no evidence that they are connected by fracture networks. On the contrary, nodules are found dispersed in the whole granitoid mass without interconnection of fractures among them. White haloes depleted in mafic minerals, when present, are limited to the neighbourhood of nodules and do not form a continuous framework connecting all nodules, as one would expect if the system was lately permeated by a B-rich fluid. The presence of white haloes, depleted in ferromagnesian components, indicates that such components may have contributed to the formation of tourmaline that became concentrated in the core of haloes. In addition, while some nodules

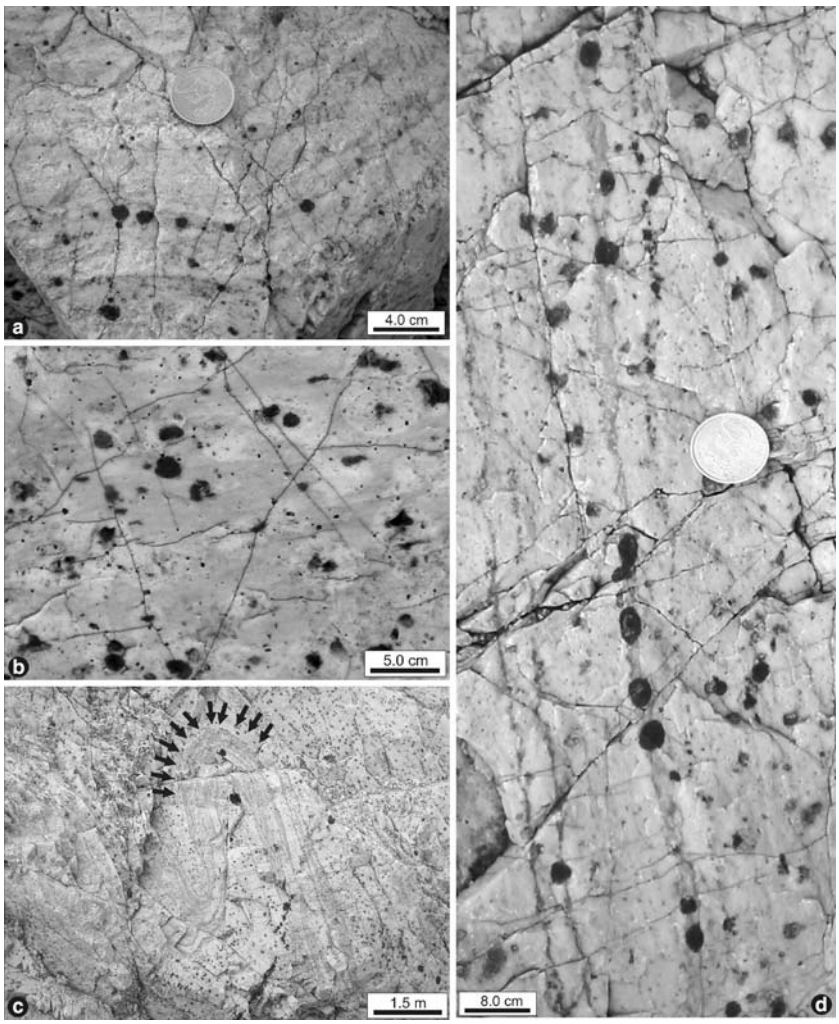

Fig. 3 **a–d** Outcrop views showing the alignment of tourmaline nodules with magmatic flow fields; **b** detailed view of the outcrop showing the occurrence of light coloured haloes depleted in ferromagnesian components around some tourmaline nodules. Note that some nodules, in the same outcrop segment, do not show any depleted halo; **c** stretched and folded magmatic structure of white and pink (*darker grey*) coloured host rock deforming the magmatic mass. *Black arrows* (upper part of the photo) indicate tourmaline nodules aligned along the fold according to the structure of magmatic flow field

have white haloes depleted in mafic minerals others do not display any halo (e.g. Fig. 3b). This occurrence is difficult to be explained with a sub-solidus growth process which would require depleted haloes to be present around all tourmaline nodules.

Another feature that would argue against the hypothesis of Rozendaal and Bruwer (1995) for explaining tourmaline nodules at Capo Bianco is the spherical nodule morphology, which is difficult to be explained by a post-magmatic, 'vein-based', replacement mechanism. In this respect, even Rozendaal and Bruwer (1995) speculate that '...the mechanism responsible for their spherical shape is not fully understood, but could relate to point nucleation at the end of dendritically arranged micro-fractures'. No evidence for such a process is present at Capo Bianco outcrop. In addition, many nodules have dendritic morphologies with outward growth direction (Fig. 5). These morphologies are typically generated by undercooling processes in liquid systems and are difficult to be explained by sub-solidus growth.

A further feature against the post-magmatic crystallization of studied tourmaline nodules is that they are commonly found aligned along streamlines that developed in the magmatic system (Figs. 2–4). This means that during motion of magma tourmaline nodules were present and they moved according to flow fields.

Therefore, according to the above discussion, it is clear that the sub-solidus hypothesis cannot be invoked to explain the occurrence of tourmaline nodules at Capo Bianco.

Sinclair and Richardson (1992) suggested a magmatic-hydrothermal origin for tourmaline nodule formation in the Seagull Batholith (Northwest Canada): (a) nodules are typically spherical in shape; (b) nodules are concentrated in the roof zone of the batholith and decrease in abundance with depth; (c) miarolitic cavities, features typically associated with late-stage volatile fluid exsolution, are present in the nodules and are locally lined with tourmaline; (d) planar structural features (i.e. veins) related to nodule development are

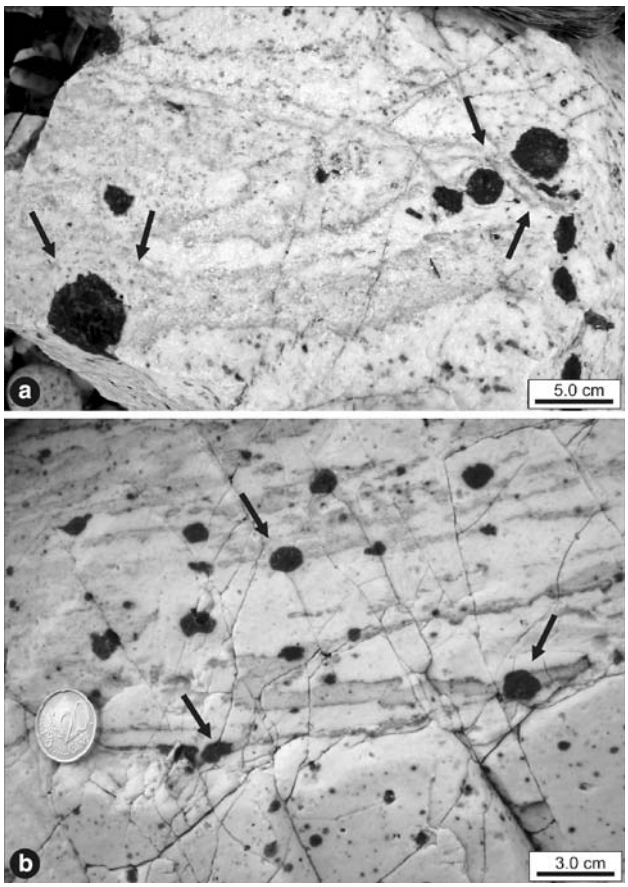

Fig. 4 Detailed view of Capo Bianco outcrop showing the deformation of magmatic flow fields around tourmaline nodules (*black arrows*; **a**) and the occurrence of tourmaline nodules (*black arrows*) cross-cutting the boundary between the white (depleted in ferromagnesian components) and pink (not depleted in ferromagnesian components; *darker grey*) coloured aplitic host rock (**b**)

lacking. Based on these features, Sinclair and Richardson (1992) proposed that a 'pocket-based' low pressure fluid exsolution theory best explained the formation of nodule morphologies and textures observed. This hypothesis has been also invoked by Shewfelt et al. (2005) to explain tourmaline nodule formation in the Scrubber Granite (Gascoyne Complex, Western Australia).

Miarolitic cavities are not observed at Capo Bianco outcrop. On the contrary, tourmaline nodules are very compact and do not show any fluid exsolution process. In addition, they do not show any petrographic and chemical internal zoning (Dini et al. 2006) as one would expect if they were the product of crystallization from fluid pockets.

Therefore it seems reasonable that the fluid pocket exsolution model of Sinclair and Richardson (1992) does not fully apply to Capo Bianco outcrop.

A third hypothesis that can be invoked to explain the presence of tourmaline nodules at Capo Bianco is that nodules may result from crystallization from a B-rich granitoid magmatic mass.

A first feature in keeping with a magmatic origin, is that nodules are commonly found aligned along streamlines that developed in the magmatic system (Figs. 2–4). This means that tourmaline nodules were present during motion of the magma and they moved according to flow fields. That tourmaline nodules were present in the magmatic mass while it was still behaving as a liquid is also well evidenced by the fact that commonly flow fields are found to fold around tourmaline nodules (Fig. 4a).

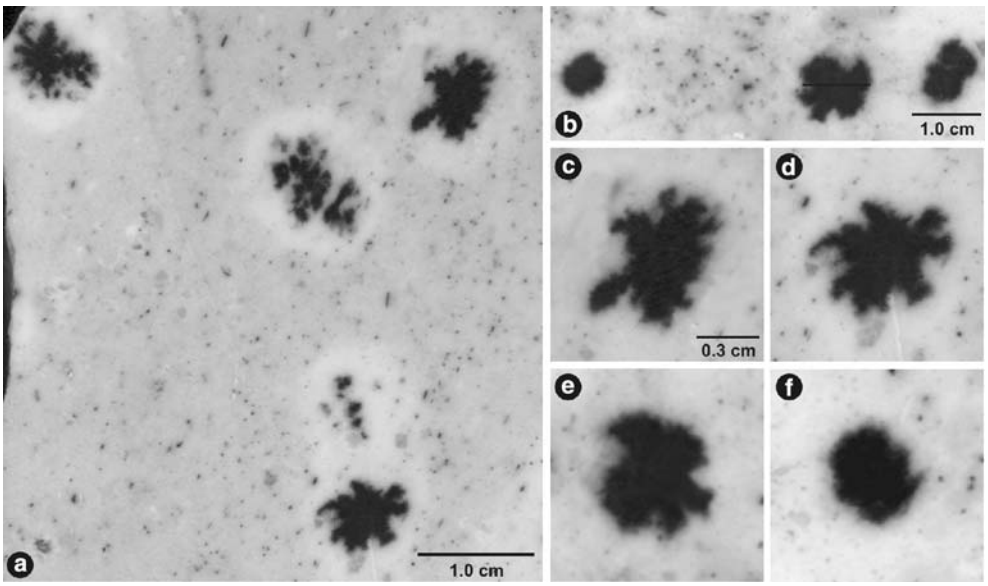

Fig. 5 Examples of tourmaline nodules with different morphologies occurring in the Capo Bianco aplite. In the centre of **a** are present disjointed nodules resulting from the sectioning of outer borders of whole nodules; of course, these nodules have been not considered in the analyses

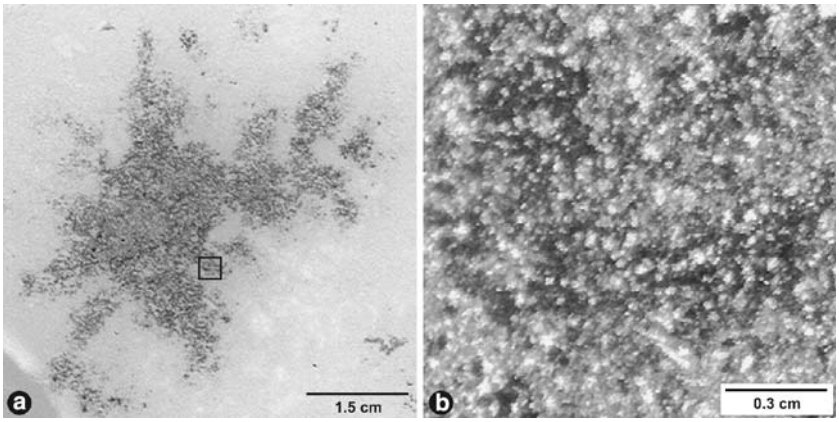

Fig. 6 **a** Example of a tourmaline nodule in thin section (plane-polarized light) showing the presence of many lacunae filled by microcrystals (**b**); **b** enlargement of the portion of (**a**) indicated by the *black square* in (**a**) showing the simultaneous extinction of the different tourmaline segments (*darkest areas* in the figure; cross-polarized light)

In addition, many nodules display an irregular morphology with fingers propagating radially from the centre of the nodule toward the host rock (Fig. 5). This morphology is typically associated with crystallization from undercooled melts, corroborating a magmatic origin for tourmaline nodules at Capo Bianco.

Another feature that may argue in favour of crystallization of tourmaline nodules from the granitoid magmatic mass is the presence of depleted haloes. Haloes can be explained by considering the growth of nodules in a magmatic system whose fluid-dynamics is governed by chaotic flow fields characterized by different dynamic regions deforming the magmatic mass. Magmatic systems are constituted by Active Mixing Regions (AMR) and Coherent Regions (CR) characterized by efficient and inefficient stretching and folding dynamics, respectively (e.g. Flinders and Clemens 1996; Perugini et al. 2002; 2003a). These can strongly influence the transport and distribution of crystals (e.g. Perugini et al. 2003b). Crystals trapped within CR do not experience strong stretching and folding processes and they remain in CR, whereas crystals in AMR are vigorously transported by flow fields (i.e. they experience strong stretching and folding dynamics), and move more erratically in the magmatic system (e.g. Perugini et al. 2003b). It is very likely that all tourmaline nodules developed a depleted halo during their growth, but, because of the presence of flow fields in the magmatic system, they underwent very different dynamic histories depending on their position in CR or AMR. In particular, if tourmaline nodules were trapped in CR, their haloes would have been preserved since the weak stretching and folding dynamics did not allow these haloes to be destroyed by flow fields. On the contrary, if tourmaline nodules were in AMR, efficient stretching and folding dynamics would have strongly deformed haloes allowing nodules to escape from those magma volumes and to migrate in other portions of the system. In these dynamic conditions haloes may have been destroyed. The latter possibility is strongly corroborated by observation of Capo Bianco outcrop where the white coloured host rock, having the same mineralogical composition as the white haloes observed around some nodules, experienced stretching and folding dynamics, as evidenced by magmatic folding of white portions and alternate lamellae of white and pink coloured rock portions (Figs. 2–4). This occurrence can be readily explained by considering the development of chaotic dynamic in the magmatic mass, as extensively recognized in magmatic systems.

In the dynamic context hypothesized above, tourmaline nodules in AMR may have passed from the white (depleted) to the pink (not depleted) portion of the host magma and this is evidenced at Capo Bianco by the presence of some nodules cross-cutting the boundary between the white and pink coloured host rock (Fig. 4). This kind of feature is commonly observed during mixing between mafic and felsic magmas in the plutonic environment, where phenocrysts (e.g. feldspars) belonging to the felsic host magma are found cross-cutting the boundary of Mafic Microgranular Enclaves (MME; e.g. Didier and Barbarin 1991 and references therein; Perugini et al. 2003c).

Therefore, considering all the above discussion our preferred genetic hypothesis for studied tourmaline nodules is that they likely represent the result of syn-magmatic crystallization from the host granitoid magmatic liquid which underwent undercooling processes and whose dynamics was governed by chaotic flow fields. The main question now arises as to what physical processes may have generated the observed morphological variability in tourmaline nodules; a possible approach may rely on morphometric analysis.

Quantitative analysis of tourmaline nodule morphology

In recent years one of the most useful approaches to measure morphological features of natural shapes has been 'fractal geometry' (e.g. Mandelbrot 1982). Fractal geometry allows us to study irregular 'objects' that cannot be adequately investigated by classical Euclidean geometry and, in particular, fractal analysis allows us to estimate a fundamental parameter, the 'fractal dimension', which quantifies the degree of irregularity of a given structure. Fractal analysis has been proven to unravel processes that could not be studied by classical petrologic techniques and, in particular, application of fractal geometry to the study of magmatic systems has shown that magmatic processes behave as chaotic systems (e.g. Flinders and Clemens 1996; Perugini and Poli 2000), thus, opening a new field of petrological research based on the combined study of classic petrological models and system dynamics (e.g. Perugini and Poli 2005; Perugini et al. 2003a, 2005).

In order to quantify the degree of complexity of tourmaline nodule morphology by fractal analysis, polished sections of rock samples were scanned with a resolution of 1pixel = 0.8 mm; then, greyscale pictures (Fig. 7a) were processed by using NIH (National Institutes of Health) image analysis software to produce binary images in which nodules and host rock were replaced by black and white, respectively (Fig. 7b). The technique used to measure the fractal dimension is known as the Box-Counting Method (BCM): a square mesh of size (r) is laid over the image and the number of boxes [$N(r)$] containing the black pixels associated with the interface between fluids is counted (Fig. 7b–d). Mandelbrot (1982) showed that, for fractal patterns, the following power-law relationship is satisfied:

$$N(r) = r^{-D_{\text{box}}} \tag{1}$$

Taking logarithms, Eq. 1 may also be written as follows:

$$\text{Log}(N_r) = -D_{\text{box}} \cdot \text{Log}(r) \tag{2}$$

Figure 7e shows the variation of $N(r)$ against r for the tourmaline nodule in Fig. 7a–d and displays that a power-law scaling may be suitable for explaining this variation, according to Eq. 1. The fractal character of tourmaline nodules is more clear in the graph of Fig. 7f where, according to Eq. 2, Log[$N(r)$] against Log(r) is shown: in the plot, data points follow a straight line ($r^2 = 0.99$) in agreement with a fractal distribution. Note that the fractal scaling range of analysed tourmaline nodules spans over ca. 1.2 orders of magnitude (from ca. 60 to 3 pixels). This scaling range is typical of empirical fractals and is in agreement with fractal analyses in the literature (e.g. Avnir et al. 1998). Below 3 pixels, strong deviations from a straight line are observed, indicating that this resolution has to be considered as the lower limit of fractal scaling for studied shapes. The fractal dimension (D_{box}) is calculated by performing a linear interpolation of the Log(r) versus Log[$N(r)$] graph, and the slope of the linear interpolation is equal to $-D_{\text{box}}$ (Fig. 7f). To estimate the uncertainty of D_{box} due to the reduction of the original greyscale images to black and white images, several measurements of the fractal dimension were performed on binary images at various threshold values. Results show that D_{box} can be estimated with an error better than 0.5%. D_{box} was measured for ninety tourmaline nodules and results show that fractal dimension ranges from 1.78 to 1.93 with more regular nodules having the highest values of D_{box}.

Growth simulation of tourmaline nodules

Macroscopic and microscopic observations and quantitative morphological analysis indicate that tourmaline nodules were generated by a growth process producing fractal morphologies with a large variability, from ca. rounded to highly irregular with 'fingers' propagating radially from the centre of the nodule towards the host rock. On this respect, any attempt to simulate the growth of studied tourmalines must result in the generation of a variety of morphologies consistent with those observed in studied samples.

Tourmaline morphologies are extremely similar to those generated by a growth process known as Diffusion-Limited Aggregation (DLA; e.g. Vicsek 1992). Formally, such a growth process starts with a seed particle at some position (x, y) on a $2D$ domain (call this set C_1). A random particle (x_0) is chosen to lie on a circle of radius R centred at point (x, y) and it is allowed to move through Brownian motion (random walk), where each step of the particle in the $2D$ domain is $x_t = B(t)$. Considering this configuration, the following metric can be defined:

$$d(x, C) = \inf\{|x - y|, y \in C\} \tag{3}$$

Then, we impose the condition that if given some small ε, i.e. a small neighbourhood in the vicinity of the existing cluster, $d(x, C_n) < \varepsilon$, $C_{n+1} = C_n \cup \{x\}$ and the

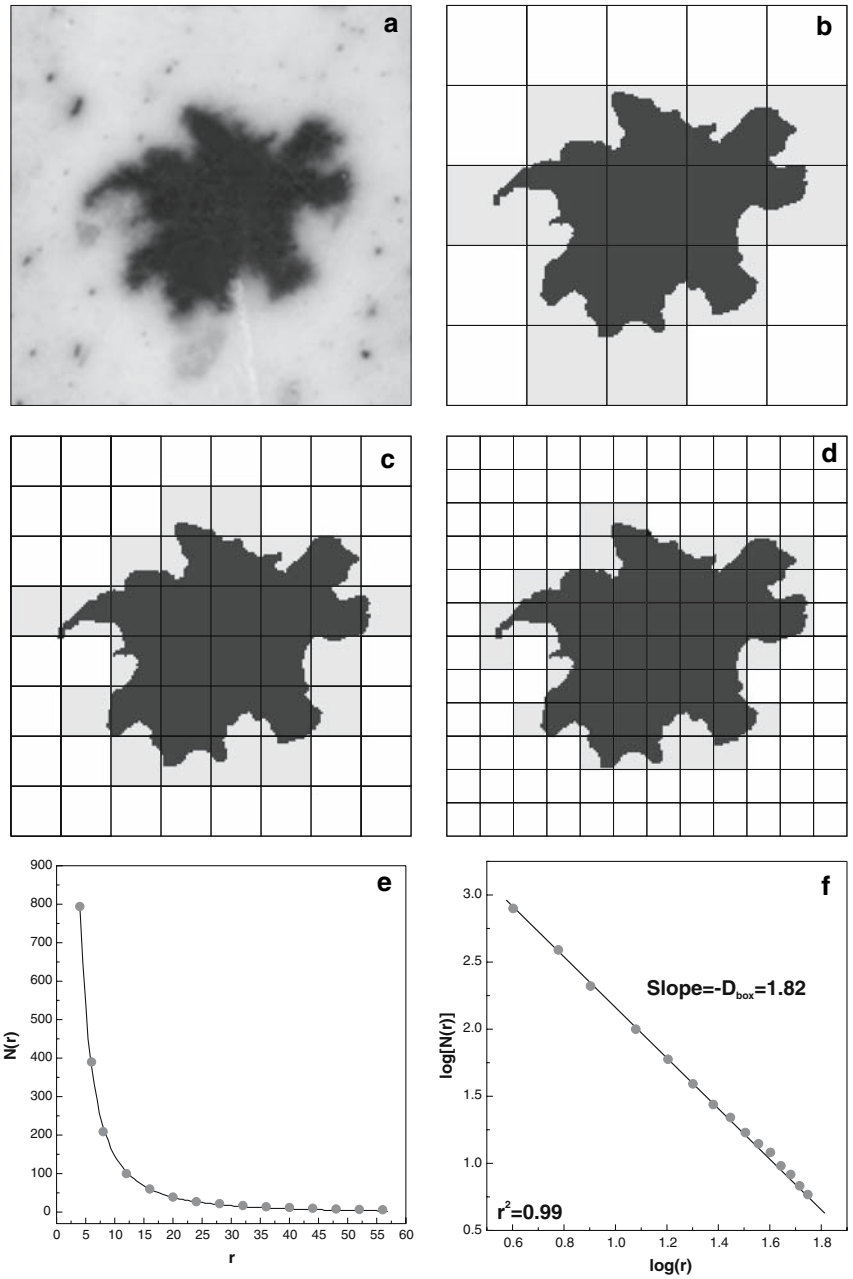

Fig. 7 **a** Original grayscale image; **b–d** binary image of (**a**), on which D_{box} has been measured; a square mesh of various sizes (r) is laid over image, and number of boxes [$N(r)$] containing black pixels associated with nodule is counted; **e** power-law relationship between r and $N(r)$ indicating the fractal character of the nodule; (f) fractal dimension (D_{box}), calculated by linear interpolation of Log(r) versus Log[$N(r)$] graph; slope of linear interpolation is equal to $-D_{box}$

new cluster is C_{n+1}. In other words, a particle diffuses via a random walk process and, if it is within some tolerance of the already existing cluster, it is incorporated into the cluster itself. Iteration of this process induces the growth of nodules with different morphologies depending on the model parameters (see e.g. Vicsek 1992 for a comprehensive review of *DLA* methods). In order to visualize the basic properties of *DLA*, the process is schematically illustrated in Fig. 8.

Several authors have shown that *DLA* growth processes can generate a variety of morphologies including rounded and irregular fractal morphologies as those observed and measured for tourmaline nodules in studied samples (e.g. Vicsek 1992; Ferreira 1994). For example, the *DLA* approach has been found to be extremely useful to study the formation of the greatly variable morphologies of snowflakes by considering different degrees of undercooling in the modelled systems (e.g. Vicsek 1992; Goold et al. 2005). The morphology resulting from a *DLA* growth process basically depends on the so-called sticking probability $p(n)$ $[0 \le p(n) \le 1]$ of particles: the higher $p(n)$, the higher the irregularity of the morphology, evolving towards a dendritic fractal pattern. In practice, $p(n)$ is

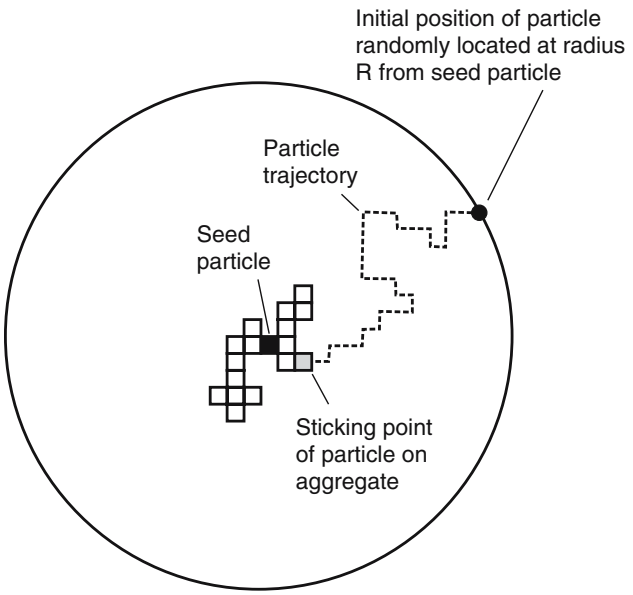

Fig. 8 Schematic illustration of the basic principles defining the Diffusion-Limited Aggregation (*DLA*) model used to simulate tourmaline nodule growth. A particle moves by random walk from the reference circle (*R*) and when it sticks to the seed particle positioned at the centre of the figure, it becomes part of the aggregate

the probability that a moving particle has to be incorporated into the growing cluster. As an example, if $p(n) = 1$ the particle sticks to the growing cluster as soon as it touches it once, whereas, if $p(n) = 0.1$ the particle has to hit the aggregate ten times before it is included in it. The result is that the higher the number of collisions that a particle experiences with the cluster, the more rounded the cluster.

As shown by several authors (e.g. Witten and Sander 1981; Vicsek 1985), the *DLA* approach allows formation of patterns by growing interfaces and such behaviour is exhibited during solidification, when a crystalline phase grows in an undercooled melt. In particular, the motion of a solidification front is determined by the diffusion field at the point x at time t, $u(x,t)$, which satisfies the equation

$$\Delta u(x,t) = 0 \tag{4}$$

As demonstrated by Witten and Sanders (1981; 1983) for *DLA*, the probability that a random walking particle released far from the interface is at the point x at time t obeys the discrete version of Eq. 4 and, therefore, diffusion-limited aggregation (*DLA*) models are suitable to simulate solidification patterns (e.g. Vicsek 1985). As discussed above, field and petrographic evidence indicates that tourmaline nodules studied in this paper can be conceived as the result of solidification from a magmatic mass and, therefore, the use of *DLA* approach may help to shed light on the processes responsible for their formation. In the context of the *DLA* process, we assume that particles sticking to form tourmaline aggregates contain all essential components necessary for tourmaline nodule formation. In this way, the problem that one element (i.e. the slowest one) would be a rate-limiting factor is bypassed by assuming that, when a new particle sticks to the aggregate, it contains all necessary components for tourmaline growth. A possible complication is the development of a boundary layer around growing crystals (e.g. Lasaga 1998). Given that Capo Bianco outcrops display typical features of chaotic systems (i.e. stretching and folding, lamellar structures), and that chaotic dynamics generate a fractal cascade of flow fields that develop from the meter to the micrometer scale, it appears reasonable to assume that boundary layers would have played only a very minor role, if any. In fact, even assuming that boundary layers may have developed around growing tourmaline crystals, they would have been suddenly destroyed by flow fields.

In order to make the *DLA* approach a physical process, Eq. 4 was solved by taking into account the following form of the Gibbs-Thomson relation (e.g. Vicsek 1985)

$$T_{\text{int}} = T_{\text{M}}\left(1 - \frac{\gamma K}{H}\right) \tag{5}$$

where T_{int} and T_{M} is the interface and melting temperature, respectively, γ is the surface tension, K is the local curvature of the interface, and H is the latent heat of crystallization.

To simulate the effects of the Gibbs-Thomson condition, Vicsek (1985) modified the original *DLA* model by considering that the probability of sticking to the surface of the aggregate depends on the local curvature of the interface. In particular, it was shown that a measure of the local surface curvature at the point x in the two-dimensional simulations is given by the number of particles (N_L) which belong to the aggregate and are within a cell of size $L \times L$ centred at point x. Assuming that changes in the shape of the surface take place on a larger scale than L, the quantity n_L-n_0 can be considered as an estimate of the average local curvature, where $n_L = N_L/L^2$ and $n_0 = (L–1)/2L$ (Vicsek 1985). Vicsek (1985) showed that the dependence of sticking probability $p(n)$ on curvature K (represented by the normalized number of particles n within the box surrounding the place of arrival at the interface) can be expressed as

$$p(n) = A(n - n_0) + B \quad (6)$$

where A and B are constants. It is possible to establish a connection between this approach and the Gibbs-Thomson equation by writing Eq. 6 as

$$p(n) = B\left[1 - \frac{A}{B}(n_0 - n)\right] \quad (7)$$

which is the same as Eq. 5 with $B = T_M$, $A/B = \gamma/H$, and n_0–$n = K$ (Vicsek 1985). In the simulations, if Eq. 7 gives $p(n) > 1$, then $p(n) = 1$ is used. In addition, when $p(n)$ is less than 0.01, the value of $p(n) = 0.01$ is taken. As shown by Vicsek (1985), the use of these approximations does not influence significantly the outcome of simulations. In the simulations, the size of cell L at the surface, in which the number of particles belonging to the cluster N_L was counted, is equal to 11, meaning that each time a particle sticks to the aggregate, 121 sites are monitored to obtain information about the local surface curvature (Vicsek 1985).

Application of the above numerical method to the problem of solidification has a number of advantages: (a) the numerical method is simple and effective, and complex geometries can be easily generated (see below), (b) the fluctuations which are always present in a thermodynamical system, and play an important role during the growth process, are included in a natural way through the random walk of the particles.

It is important to note that the value of $p(n)$, the parameter governing the *DLA* growth process, depends on values of curvature (K), A, and B. Curvature (K) is a feature inherent to the growing shape and cannot be regulated a priori. On the contrary, A and B can be chosen at the beginning of the simulations, and they basically control the growth mechanism. As shown above, the A/B ratio equals the ratio between surface tension (γ) and latent heat (H) and, since these two are the fundamental parameters controlling the solidification process in an undercooled melt, they play a role of great importance. For this reason, in the numerical simulations that will be presented below, we will focus on the A/B ratio to evaluate its influence on the outcome (i.e. simulated nodule morphologies). More extensive comments about significance of A/B in the studied system will be given in the Discussion section.

Figure 9a–f shows the outcome of *DLA* simulations performed by considering 2.0×10^5 particles for different values of the A/B ratio. It is shown that passing from low ($A/B = 2.0$) to high ratios ($A/B = 60.0$), the morphology of the nodule moves from highly dendritic (Fig. 9a), similar to typical manganese deposits in limestone, towards less irregular and rounded (Fig. 9f). Comparison between simulated nodules (Fig. 9a–f) and tourmaline nodules in natural samples (Fig. 5) shows a striking similarity of morphologies, especially for those simulations performed with A/B ratios in the range $4.0 \le A/B \le 60.0$. In natural samples, highly dendritic structures, as those obtained for A/B ratios lower than 4.0, do not occur, indicating that such growth mechanisms are not likely to have acted in the studied natural system.

Analogous to the natural case, the fractal dimension (D_{box}) of simulated tourmaline nodules has been measured by the Box-Counting Method [BCM; Eq. 1 and 2] and Fig. 9g displays the variation of D_{box} against the A/B ratio. It is shown that the degree of irregularity (D_{box}) of nodule morphology decreases (higher D_{box} values) as the A/B ratio increases; in detail, D_{box} values show an asymptotic saturation towards a $2D$ Euclidean surface (i.e. $D_{box} = 2.0$) as A/B increases. Note that D_{box} values measured for simulated structures (D_{box} from 1.74 to 1.94) overlap the range of values measured on natural samples (D_{box} from 1.78 to 1.93), corroborating the hypothesis that natural tourmaline nodules may be the result of a *DLA* growth mechanism.

An additional important feature shown by the simulations is the presence of lacunae in the simulated nodules (white small areas in the black shapes of Fig. 9d–f). As reported above, the presence of lacunae was also observed in natural tourmaline nodules (Fig. 6), again indicating a strong convergence between natural samples and numerical simulations. The presence of such lacunae can be explained by considering the screening effect exerted by local growing structures in time. Figure 10 shows a schematic representation of this screening effect. In detail, once the nodule starts to grow, it develops small tips bulging into the liquid phase (Fig. 10a); as the process progresses in time these tips become potential points of attachment for diffusing particles and the structure may becomes locally ramified (Fig. 10b). The progression of this process in time may lead to coalescence of growing tips (Fig. 10c), thus precluding particles to penetrate into those regions that remain isolated (dashed areas in Fig. 10c), and forming the lacunae that we now observe in both simulated and natural tourmaline nodules.

Therefore, in conclusion, qualitative observations (i.e. nodule morphology and presence of lacunae) and quantitative analysis (i.e. measurement of fractal dimension, D_{box}) argue in favour of the hypothesis that natural tourmaline nodules may represent an example of Diffusion-Limited Aggregation (*DLA*) growth in a magmatic systems.

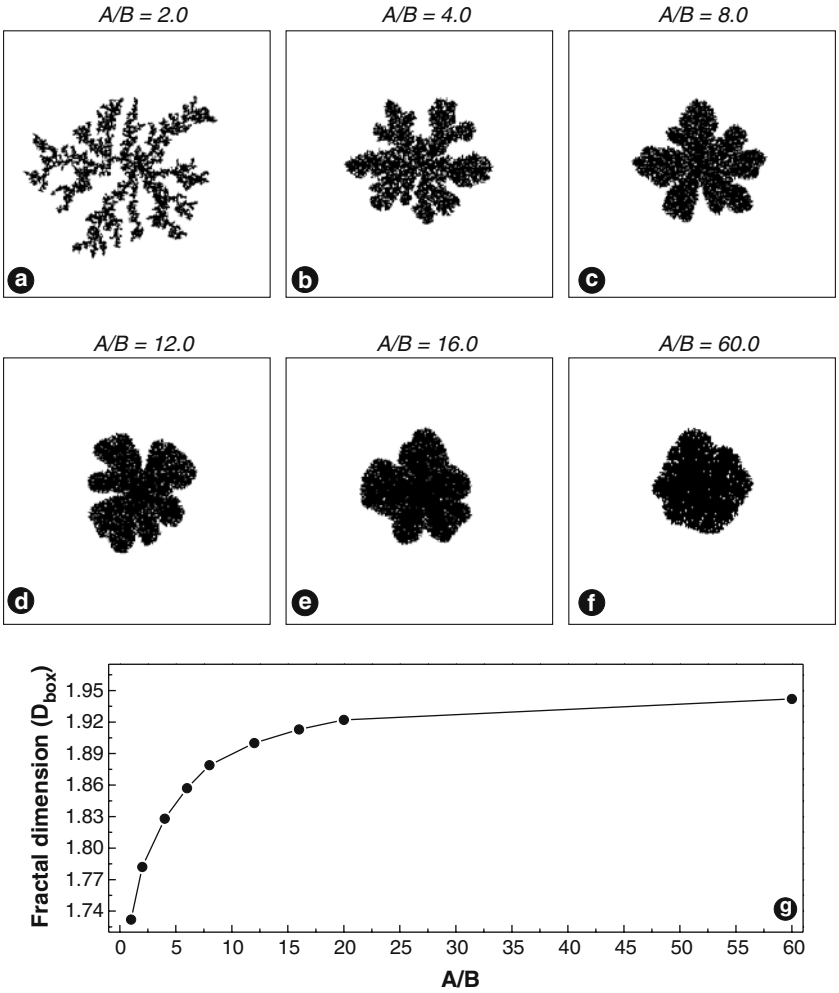

Fig. 9 **a–f** Tourmaline nodules simulated by the *DLA* model with different values of the A/B ratio. Passing from (**a**) to (**f**) the roundness of the nodule increases (i.e. D_{box} increases); **g** dependence of fractal dimension (D_{box}) on the A/B ratio for the simulated tourmaline nodules

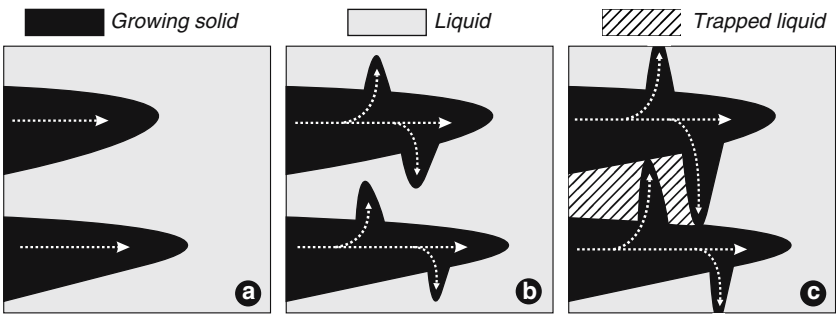

Fig. 10 Schematic representation of the screening effect exerted by local growing structures on particle diffusion resulting in the production of lacunae in the nodules. Growth time increases from (**a**) to (**c**)

The main question now arises as to what physico-chemical conditions may have induced the development of different morphologies, having variable degree of irregularity, in the studied natural samples.

Discussion

In the attempt of addressing the above question, we must recall that the factor controlling the morphology of nodules in the simulations is the ratio A/B. As previously discussed, this ratio is analogous to the ratio γ/H [i.e. (surface tension)/(latent heat)] and, therefore, we can discuss the relative role played by γ and H on the development of variable morphologies. Regarding γ, commonly, crystalline phases display variable values of γ depending on the crystallographic orientation of dihedral faces and, in general, high surface tension corresponds to high surface energy (e.g. Pimpinelli and Villain 1999). During crystal growth, surface energy

tends to be minimized because, according to Gibbs law of free energy, total free energy in the system needs to be kept at minimum. In order to account for this thermodynamical requirement, faces with high surface energy grow less relative to faces with low surface energy. Accordingly, during a solidification process in which surface tension plays an important role (i.e. surface energy is the limiting growth factor) directional solidification fronts are necessarily developed inducing a preferential growth along well defined directions. Observation of natural tourmaline nodules clearly indicates that they all have a morphology strongly associated with a spherical symmetry with a centre corresponding to the centre of gravity of each nodule. This is valid not only for rounded nodules, but also for nodules exhibiting fingered morphologies, because such fingers radiate from the centre of gravity of the nodule. This observation indicates that surface tension played only a minor role, if any, in the development of tourmaline nodule morphologies. If the growth process was surface controlled, fingers would have been developed along a limited number of preferential directions and not radially from a common centre towards any direction, contrary to that observed in natural samples.

This being so, the causes of the variable nodule morphologies in the studied magmatic system should be associated to the other factor controlling the magnitude of the A/B ratio, i.e. parameter H (latent heat of crystallization). In this respect, during solidification from an undercooled melt, as in the case hypothesized in this paper, latent heat is progressively released at the crystal/liquid interface and this induces a fluid dynamic instability promoting the onset of local convection dynamics across the heated boundary layer and the nearby liquid mass (e.g. Nagatani 1988). By using the renormalization-group approach applied to the DLA solidification process, Nagatani (1988) has shown that the latent heat flux is increased by stronger convection dynamics as the growth rate of the interface increases for solidification from an undercooled melt. In particular, at places where the growth rate is larger the latent heat flux is increased more than at places with smaller growth rate. In such conditions, convection acts as a destabilizing force which enhances the roughness of the interface, generating progressively more irregular morphologies as the strength of convection increases.

These considerations would explain the presence of tourmaline nodules with variable morphologies, depending on the growth rate of single nodules. Although this is a satisfactory explanation for justifying the different nodule morphologies, it does not explain why so morphologically different nodules are found side by side in the magmatic mass.

As discussed above, the basic parameter controlling the morphology of tourmaline nodules is the growth rate of individual nodules. Therefore, to generate different morphologies in the same system, different growth rates must be invoked for nodules growing at short length scale. This implies that some additional factors should have played a role in regulating the growth rate of individual tourmaline nodules.

As discussed in the first part of the paper (Tourmaline nodules from Capo Bianco aplite (Elba Island, Italy) and Hypotheses for tourmaline nodule formation), Capo Bianco outcrop displays the presence of stretching and folding dynamics in the magmatic mass as evidenced by the occurrence of lamellae and folds along which tourmaline nodules were transported. As stated, stretching and folding dynamics generate different dynamical regions, characterized by strongly different dynamics in the same system at short length scale, down to the order of a single thin section (e.g. Perugini et al. 2002, 2003a). This feature has been proven to be strictly connected to the development Active Mixing Regions (AMR) and Coherent Regions (CR) in the same system (e.g. Perugini et al. 2002, 2003a). In such dynamic conditions, where flow fields are strongly variable in space, scalar quantities such as concentration of nutrient elements available for crystal growth can be greatly influenced by flow fields (e.g. Perugini et al. 2002, 2003a). Thus, according to the studied natural outcrop, where stretching and folding dynamics have been observed, the analysis of the structure of flow fields in the magmatic mass may help in explaining the development of the varied tourmaline nodule morphologies in relationship to the transfer of nutrients.

Stretching and folding are non-linearly coupled processes. The first induces elongation of melts whereas the latter bends and redistributes them through the system. As shown by several authors (e.g. Ottino 1989; Muzzio et al. 1992; Liu et al. 1994; Aref and El Naschie 1995), efficient stretching and folding dynamics are typically associated with AMR, whereas weak stretching and folding processes promote the formation of CR. The development of chaotic and regular regions into a fluid dynamic system can be better understood by considering a prototypical numerical system widely used in fluid dynamic simulations (e.g. Liu et al. 1994; Clifford et al. 1998; 1999) and that has been proven to apply well to magmatic systems (e.g. Perugini et al. 2003a; Perugini et al. 2004). The model is known as the sine-flow map and has the following formulation on a $2D$ domain:

$$x_{n+1} = x_n + \frac{k}{2} \cdot \sin(2\pi \cdot y_n) \quad [\text{mod}1]$$
$$y_{n+1} = y_n + \frac{k}{2} \cdot \sin(2\pi \cdot x_{n+1}) \quad [\text{mod}1] \tag{8}$$

It forms a two-dimensional conservative (area preserving) chaotic system whose domain is $0 \le (x, y) \le 1$ and where k is the parameter of the map. From a kinematical point of view, the flow is the combination of two orthogonal motions, each with a sinusoidal velocity profile. The flow is defined on the $2D$ torus meaning that whenever a particle exits the unit square, it re-enters the box through the opposite side. This flow scheme induces motion of a fluid mass by stretching and folding, and is composed of CR and AMR (details on this flow scheme and its applicability to magmatic systems can be found in Perugini et al. 2003a, 2004). In the following the sine-flow dynamical system with a value of $k = 0.4$ is used. Changing k in the range of 0.1–0.6 (i.e. when both CR and AMR are present in the system) does not significantly influence presented results. Figure 11a shows the Poincaré section for the sine-flow map, that corresponds to the flow fields in the system (see Perugini et al. 2003a). The image shows that regions consisting of closed trajectories coexist with regions where precise trajectories cannot be defined and where the points are distributed irregularly. Bearing in mind that the efficiency of mass transport in the system lies in the ability of the components involved to spread across the system, possibly in an irregular way (e.g. Ottino 1989; Liu et al. 1994), it follows that system volumes characterized by close orbits and irregular points are regions where mass transport occurs inefficiently (weak stretching and folding) and efficiently (strong stretching and folding), respectively.

As pointed out by several authors (e.g. Ottino 1989; Ferrachat and Ricard 1998; Farnetani and Samuel 2003), a more rigorous and useful characterization of the flow can be achieved by estimating the Lyapunov exponent. The Lyapunov exponent is an indicator of the sensitivity to small perturbations of the initial position, and provides a quantitative measure about the chaoticity of the system (Farnetani and Samuel 2003). In detail, the higher the Lyapunov exponent, the higher is the chaoticity of the system (e.g. Ottino 1989; Ott 1994). If we consider a pair of fluid particles at an initial distance $\delta_0(x,y,0)$ and we track the distance $\delta(x, y, \hat{t})$ between their trajectories, after a time τ, the Lyapunov exponent is defined by:

$$\lambda = \lim_{\substack{t\to\infty \\ \delta_0\to 0}} \left[\frac{1}{\hat{t}} \ln\left(\frac{\delta}{\delta_0}\right)\right] \tag{9}$$

For practical purposes, we can follow the distance $\delta(x, y, \hat{t})$ between couples of tracers initially located at very close distance $\delta_0(x,y,0)$. In this case the Lyapunov exponent is approximated by:

$$\lambda = \frac{1}{\hat{t}} \ln\left(\frac{\delta}{\delta_0}\right) \tag{10}$$

and described as the 'finite time Lyapunov Exponent' (e.g. Ferrachat and Ricard 1998; Farnetani and Samuel 2003). The Lyapunov exponent can be conceived as a measure of divergence on nearby flow orbits and, therefore, it is a parameter which quantifies the ability of the system to redistribute any scalar quantity in the system, such as concentration of nutrient elements needed by growing tourmaline nodules.

The graph of Fig. 11b shows the spatial distribution of normalized Lyapunov exponents [Log(λ)] in the sine-flow dynamical system for $k = 0.4$. It is shown that the system is characterized by a large region of high λ values in which four regions having lower λ values are immersed. These features are also seen in the frequency histogram of Fig. 11c where it is clear that a bimodal distribution of Log(λ) is present, with the two peaks corresponding to regions of low and high λ values. The large region with the high λ values is the AMR in which efficient stretching and folding dynamics induce a strong divergence of nearby orbits potentially leading to efficient exchange of nutrient elements for crystal growth. On the contrary, the four small regions with low λ values are CR characterized by inefficient stretching and folding dynamics where the closed structure of flow fields inhibits efficient exchange of nutrient elements. Note that chaotic dynamical systems, such as the sine-flow map, generate fractal structures and this feature is also observed for AMR and CR that coexist at many length scales, thus governing the transfer of nutrient elements at many length scales (e.g. Perugini et al. 2003a).

The contemporaneous presence in the system of AMR and CR may act as control factor for the growth rate of tourmaline nodules and, therefore, it may offer an explanation for the presence of tourmaline nodules with variable morphologies in the same system coexisting at short length scale. In particular, if the growth of a tourmaline nodule occurs in a AMR, its growth rate is high because of the chaotic structure of the flow fields which allows efficient recharge of nutrient elements. According to Nagatani (1988), it follows that latent heat flux is high, convection dynamics are strong, and the formation of irregular morphologies is enhanced. On the contrary, if the growth of a tourmaline

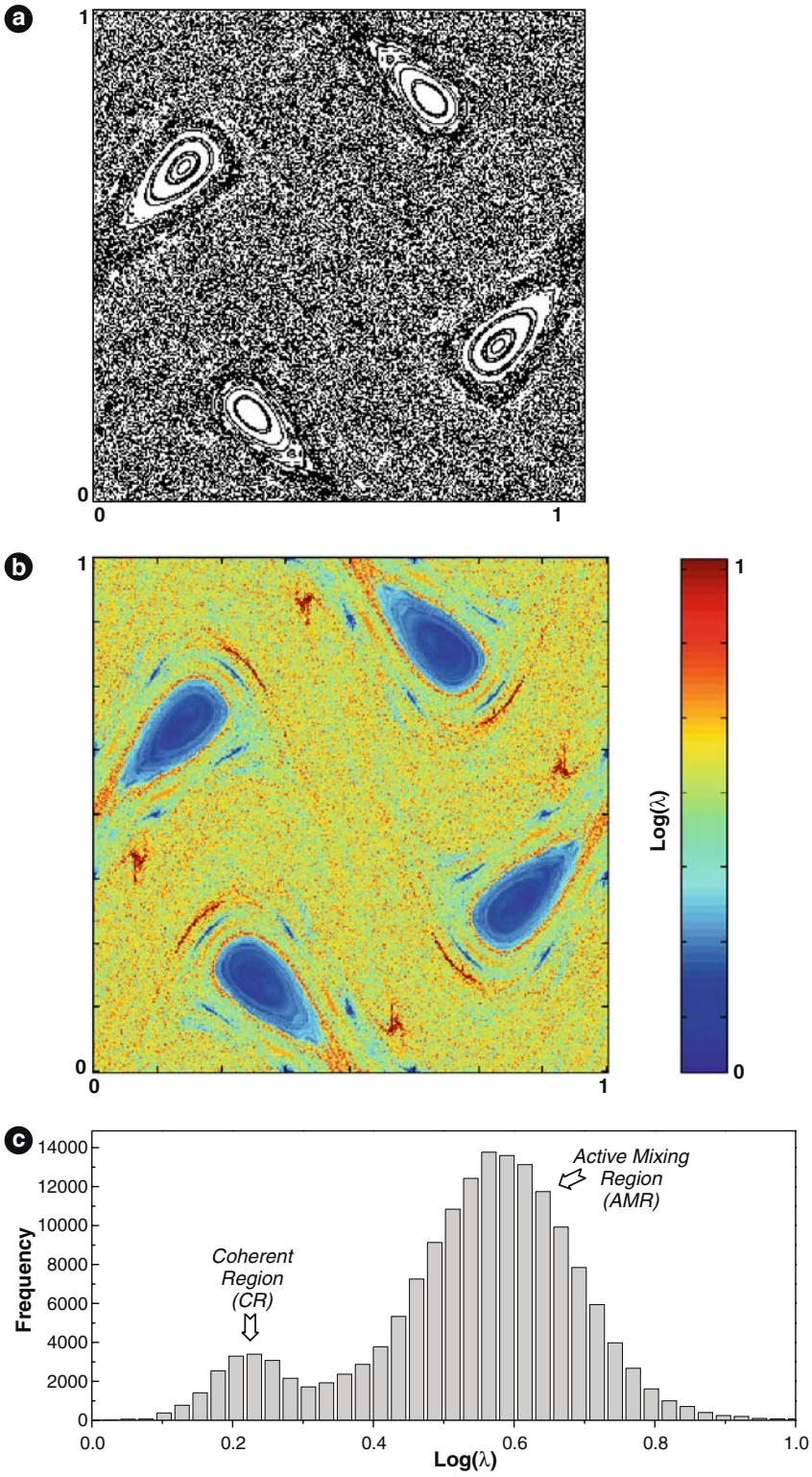

Fig. 11 **a** Poincaré map of the sine-flow for $k = 0.4$ showing the presence of two different dynamical regions constituted by closed orbits (regular regions) and dots irregularly distributed (chaotic regions); **b** spatial distribution of normalized Lyapunov exponents [Log(λ)] in the sine-flow map for $k = 0.4$; **c** frequency histogram of Lyapunov exponents [Log(λ)] for the system shown in (**b**)

nodule occurs in a CR transfer of nutrient elements is limited by the closed structure of flow fields, inducing low growth rates. In this conditions, latent heat flux is low, convection dynamics are weak, and the formation of rounded morphologies is favoured. To better capture the logic progression of the proposed model, Fig. 12 shows a diagram resuming the relationships between system dynamics and nodule growth.

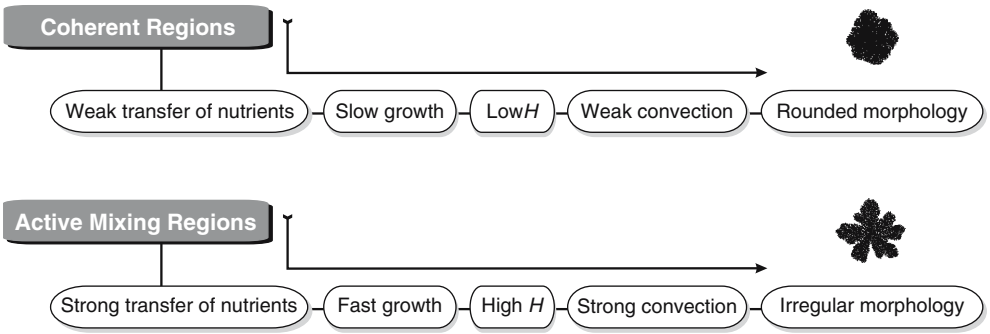

Fig. 12 Flow chart summarizing the processes hypothesized to act in the studied magmatic system and originating the variable morphologies of tourmaline nodules

Summary and conclusions

In this contribution the morphology of tourmaline nodules occurring in the Capo Bianco aplite (Elba Island, Italy) have been studied. It has been shown that tourmaline nodule morphologies are fractals and that fractal dimension can be utilized to quantify the degree of irregularity of morphologies. Nodule morphologies of natural samples have been reproduced by numerical simulations performed by Diffusion-Limited Aggregation growth processes physically scaled in order to keep into account the most important parameters acting during solidification from an undercooled melt. In detail, the proposed model includes (a) the random walk of the nutrient elements representing the fluctuations which are always present in a thermodynamical system, (b) the surface tension, and (c) the latent heat of crystallization. Results from the simulations show a strong similarity between natural and simulated samples indicating that the Diffusion-Limited Aggregation growth may have played an important role in the genesis of studied tourmaline nodules.

The presence in natural samples of nodules with different morphologies occurring at short length scale has been explained by considering a complex interplay between growth rate in different dynamical regions, latent heat of crystallization, and local convection dynamics. It is suggested that higher growth rates correspond to growth of tourmaline nodules in active mixing regions where the transfer of nutrients is very efficient. In such dynamical conditions, the latent heat released by the growing nodule is high and this induces strong local convection dynamics destabilizing the nodule interface and promoting the formation of irregular morphologies. On the contrary, growth of tourmaline nodules in coherent regions may be inhibited because of weak transfer of nutrients leading to weak local convection dynamics and, consequently, to the formation of rounded morphologies.

In conclusion, it was shown that complex textural features in igneous rocks may be explained by taking into account the typical non-linearity of magmatic processes and by including in the models, concepts and methods from non-linear physics, fractal geometry, and chaos theory. The remarkable point here is that fractal growth modelling of mineral phases can be accomplished by including physical parameters controlling the spatial and temporal evolution of the modelled system in combination with system dynamics. The approach presented in this paper may be extended to other case studies, and in particular, to the modelling of crystal morphologies in lava flows that experienced variable degrees of undercooling to extract information about the interplay between chemical evolution and dynamics experienced by the magmatic mass.

Acknowledgments We thank A. Dini for the illuminating discussions about Capo Bianco outcrops. Constructive comments of M. Elburg and N. Petford, as well as editorial handling of W. J. Collins are gratefully acknowledged. This work was funded by MIUR (Ministero dell'Istruzione, dell'Università e della Ricerca), and Università degli Studi di Perugia grants.

References

Aref H, El Naschie MS (1995) Chaos applied to fluid mixing. Pergamon Press, Reprinted from Chaos, Solutions and Fractals, 4(6), Exeter, pp 377

Avnir D, Biham O, Lidar D, Malcai O (1998) Is the geometry of nature fractal? Science 279:39–40

Cashman KV (1993) Relationship between crystallization and cooling rate: insight from textural studies of dikes. Contrib Mineral Petrol 113:126–142

Chaplain MAJ, Singh GD, McLachlan JC (1999) On growth and form: spatio-temporal pattern formation in biology. Wiley, New York, pp 436

Clifford MJ, Cox SM, Roberts EPL (1998) Lamellar modelling of reaction, diffusion and mixing in a two-dimensional flow. Chem Eng J 71:49–56

Clifford MJ, Cox SM, Roberts EPL (1999) Measuring striation widths. Phys Lett A 260:209–217

Didier J, Barbarin B (1991) Enclaves and granite petrology. Developments in petrology 13, Elsevier, Amsterdam, p 625

Dini A, Innocenti F, Rocchi S, Tonarini S, Westerman DS (2002) The magmatic evolution of the late Miocene laccolith–pluton–dyke granitic complex of Elba Island, Italy. Geol Mag 139:257–279

Dini A, Corretti A, Innocenti F, Rocchi S, Westerman DS (2006) Sooty sweat stains or tourmaline spots? The Argonauts at Elba Island (Tuscany) and the spread of Greek trading in the Mediterranean Sea. In: Piccardi L et al. (eds) Myth and geology. Geological Society of London Special Publication 273 (in press)

Farnetani CG, Samuel H (2003) Lagrangian structures and stirring in the Earth's mantle. Earth Planet Sci Lett 206:335–348

Faure F, Trolliard G, Nicollet C, Montel JM (2003) A developmental model of olivine morphology as a function of the cooling rate and the degree of undercooling. Contrib Mineral Petrol 145:251–263

Ferrachat S, Ricard Y (1998) Regular vs. chaotic mantle mixing. Earth Planet Sci Lett 155:75–86

Ferreira SC (1994) Effects of the screening breakdown in the diffusion-limited aggregation model. Eur Phys J B 42:263–269

Flinders J, Clemens JD (1996) Non-linear dynamics, chaos, complexity and enclaves in granitoid magmas. Trans R Soc Edinburgh Earth Sci 87:225–232

Goold NR, Somfai E, Ball CR (2005) Anisotropic diffusion limited aggregation in three dimensions: universality and nonuniversality. Phys Rev E 72:031403–1–10

Lasaga A (1998) Kinetic theory in the earth sciences, Princeton series in geochemistry. Princeton University Press, Princeton, New Jersey, p 811

Liu M, Muzzio FJ, Peskin RL (1994) Quantification of mixing in aperiodic chaotic flows. Chaos Solitons Fractals 4:869–893

Mandelbrot BB (1982) The fractal geometry of nature. W H Freeman, New York, pp 480

Muzzio FJ, Swanson PD, Ottino JM (1992) Mixing distributions produced by multiplicative stretching in chaotic flows. Int J Bif Chaos 2:37–50

Nagatani T (1988) Convection effect on the diffusion-limited-aggregation fractal: renormalization-group approach. Phys Rev A 37:4461–4468

Ott E (1994) Chaos in dynamical systems. Cambridge University Press, Cambridge, England, p 490

Ottino JM (1989) The kinematics of mixing: stretching, chaos and transport. Cambridge University Press, Cambridge, p 364

Ottino JM, Leong CW, Rising H, Swanson PD (1988) Morphological structures produced by mixing in chaotic flows. Nature 333:419–425

Perugini D, Poli G (2000) Chaotic dynamics and fractals in magmatic interaction processes: a different approach to the interpretation of mafic microgranular enclaves. Earth Planet Sci Lett 175:93–103

Perugini D, Poli G (2005) Viscous fingering during replenishment of felsic magma chambers by continuous inputs of mafic magmas: field evidence and fluid-mechanics experiments. Geology 33:5–8

Perugini D, Poli G, Gatta G (2002) Analysis and simulation of magma mixing processes in 3D. Lithos 65:313–330

Perugini D, Poli G, Mazzuoli R (2003a) Chaotic advection, fractals and diffusion during mixing of magmas: evidence from lava flows. J Volcanol Geoth Res 124:255–279

Perugini D, Busà T, Poli G, Nazzareni S (2003b) The role of chaotic dynamics and flow fields in the development of disequilibrium textures in volcanic rocks. J Petrol 44:733–756

Perugini D, Poli G, Christofides G, Eleftheriadis G (2003c) Magma mixing in the sithonia plutonic complex, Greece: evidence from mafic microgranular enclaves. Mineral Petrol 78:173–200

Perugini D, Ventura G, Petrelli M, Poli G (2004) Kinematic significance of morphological structures generated by mixing of magmas: a case study from Salina Island (Southern Italy). Earth Planet Sci Lett 222:1051–1066

Perugini D, Poli G, Valentini L (2005) Strange attractors in plagioclase oscillatory zoning: petrological implications. Contrib Mineral Petrol 149:482–497

Pimpinelli A, Villain J (1999) Physics of crystal growth, Cambridge University Press, p 377

Rozendaal A, Bruwer L (1995) Tourmaline nodules: indicator of hydrothermal alteration and Sn–Zn–(W) mineralization in the Cape Granite Suite, South Africa. J African Earth Sci 21:141–155

Shewfelt D, Ansdell K, Sheppard S (2005) The origin of tourmaline nodules in granites; preliminary findings from the Paleoproterozoic Scrubber Granite. Geological Survey of Western Australia Annual Review 59–63

Sinclair DW, Richardson JM (1992) Quartz–tourmaline orbicles in the Seagull Batholith, Yukon Territory. Can Mineral 30:923–935

Vicsek T (1985) Formation of solidification patterns in aggregation models. Phys Rev A 32:3084–3089

Vicsek T (1992) Fractal growth phenomena. World Scientific, Singapore, p 488

Westerman DS, Dini A, Innocenti F, Rocchi S (2000) Christmas trees in the shallow crust: the nested laccolith complex from Elba Island, Italy. Geoscience 2000, 11

Witten TA, Sander LM (1981) Diffusion-limited aggregation, a kinetic critical phenomenon. Phys Rev Lett 47:1400–1403

Witten TA, Sander LM (1983) Diffusion-limited aggregation. Phys Rev B 27:5686–5697